PREDICTION OF THE LOW-ENERGY IMPACT RESPONSE OF A SELF-REINFORCED POLYMER BASED ON A RHEOLOCIAL MODEL

J. I. Múgica[1*], L. Aretxabaleta[1], I. Ulacia[1], M. Mateos[1], J. Aurrekoetxea[1]

[1]*Mechanics and Industrial Manufacturing Department, Mondragon Goi Eskola Politeknikoa, Mondragon Unibertsitatea, Loramendi, 4, 20500 Mondragón, Guipuzcoa, Spain.*
**jimugica@mondragon.edu*

Keywords: self-reinforced polymer, polypropylene, impact, rheological model.

Abstract

In this paper, a rheological model to predict the contact force history during low-energy impacts on a self-reinforced polypropylene (SRPP) is proposed. The model consists of two subsystems; one represents and models the indentation phenomenon based on the Hertz theory, while the other one the deflection of the plate considering the bending and membrane effects based on the plates and shells theory. The parameters of the model are obtained from the mechanical properties of the material, one indentation impact test and one transverse impact test. The numerical response is compared with experimental data obtained previously for different impact heights and plate thicknesses. The results demonstrate that the model is capable of reproducing accurately the impact response of the material.

1. Introduction

Every year, end of life vehicles (ELV) generate between 8 and 9 million tonnes of waste in the European Community which should be managed correctly [1]. In response, the European Parliament and the Council officially adopted and published a legislation which established that only the 5% of ELV residues could be put into landfills [2]. Accordingly, the recyclability of materials has become a major issue in the Automotive Sector. This feature must not be put ahead of the specific mechanical properties of the materials. The reason is that vehicles are susceptible to crashes; in these situations, components must perform appropriately so that the minimum safety requirements for the occupants are complied.

Self-reinforced polymers (SRPs) (also referred to as single polymer composites or all-polymer composites) are composite materials whose main feature is that the reinforcement and the matrix belong to the same polymer family (polypropylene, polyethylene, etc.) [3]. Their fibres, which are highly oriented, provide the composite with higher strength and stiffness than those of the bulk polymeric material [4] [5]. To manufacture SRPs there are different consolidation techniques, such as film stacking [6], injection moulding [7], wet powder [8] or solution impregnation [9]. The recyclability is one of the main advantages of all-polymer composites. Moreover, SRPs have also demonstrated other interesting properties for the Automotive Sector, such as improved impact resistance, when compared to thermosetting composites [10], and capability of being thermoformed [11]. Currently, different kinds of products made of SRP have already come out to the market, always related with impact applications, such as armour, luggage and sport equipment [12] [13]. Moreover, SRP thin plates can also be combined with metal sheets to obtain fibre metal laminates (FML) offering higher specific impact resistance even than that of the plain composite [14]. In accordance with the previously described, the study of the impact responses of SRPs is justified.

Normally, when a plate is submitted to a low-velocity impact loading, two phenomena can be principally distinguished in its mechanical response; the indentation by the striker (local response) and the plate deflection (global response). One of the alternatives to reproduce these responses is using mass-spring-dashpot systems [15] [16]. Work done to date on these systems deals with relatively stiff materials, such as metals and thermosetting composites [17], when compared to all-thermoplastic composites. The indentation phenomenon is often modelled based on the Hertzian contact law and the plate deflection based on the low plate deflection theory. However, when the deflection is relatively high when compared to the thickness of the plate, membrane effect must be taken into account [15]. The possibility that this phenomenon occurs for certain impact energy is higher in SRPs than in other polymer composite materials as a consequence of their higher flexibility. Apart from this, SRPs are normally non-linear in their elastic phase [14], which determines their low-energy impact response.

In this work, a rheological model to predict the contact force history during low-energy impacts on a self-reinforced polypropylene (SRPP) is proposed. The model considers the membrane effect, as well as the bending and indentation phenomena. Moreover, an expression of the strain dependent stiffness of the material is deduced to take into account such dependence in the low-velocity impact response.

2. Theoretical background

2.1. Contact mechanics

Local deformations in the contact zone as a consequence of indentation phenomena may have a significant effect on the contact force history and must be accounted for in the analysis. Results obtained by Rayleigh [18] show that if the contact duration between the striker and the target is very long in comparison with their natural frequencies, vibrations of the system can be neglected. It can be therefore assumed that the Hertzian contact law of two elastic isotropic spheres [19], which was established for static conditions, can be appplied also during impact. A particular case is indentation, for which the radius of one of the spheres becomes infinite; then the problem becomes the contact between a sphere and a half-space. Accordingly, the relation between the contact force, F_i, and the indentation depth, x_i, can be expressed as

$$F_\mathrm{i} = k_\mathrm{i} x_\mathrm{i}^{3/2} \tag{1}$$

where k_i is defined as

$$k_\mathrm{i} = \frac{4}{3} R^{1/2} \left(\frac{1-\nu_1^2}{E_1} + \frac{1-\nu_2^2}{E_2} \right)^{-1} \tag{2}$$

where the subscripts 1 and 2 denote indenter and target, respectively, R is the radius of the indenter, ν is the Poisson's ratio and E is the Young's modulus.

The same approach can be used for investigating the more general case of impact between two arbitrary bodies of revolution made of transversely isotropic and orthotropic materials, including targets made of laminated composites. Theory extension to arbitrary bodies of revolution requires that appropriate equations corresponding to the solution of the contact problem between such bodies be used.

Although no closed-form solution has been found for k_i for generally orthotropic solids and its derivation appears to be extremely complex, an approximate numerical solution for k_i of generally orthotropic solids shows k_i to be relatively insensitive to the in-plane fibre orientation [20]. As noted by Greszczuk [20], the properties that influence k_i the most are those associated with the thickness direction, that is, the direction of impact, *z*. Because of the weak dependence of k_i on the in-plane properties of the target, the approach for transversely isotropic materials can, as a first approximation, be used for generally orthotropic materials if appropriate, say average, in-plane properties are used.

The 3/2 power law given by Eq. (1) was found to be valid by Willis [21] for a rigid sphere pressed on a transversely isotropic half-space and he deduced a modified contact law for composite materials with

$$k_i = \frac{4}{3} R^{1/2} \left(\frac{1-\nu_1^2}{E_1} + \frac{1}{E_{t2}} \right)^{-1} \tag{3}$$

where E_{t2} is the Young's modulus of the composite target in the direction normal to the contact plane.

2.2. Rheological models

Spring-mass models are simple and provide accurate solutions for some types of impacts often encountered during tests on small size specimens. The most complete conservative model consists of one linear spring representing the bending and shear stiffnesses of the structure, k_b and k_s, respectively (joined, k_{bs}); another non-linear spring for the membrane stiffness, k_m; a mass, m_{eff}, representing the effective mass of the structure; a non-linear spring for contact stiffness, k_i; and a mass, m_t, representing the striker [15]. However, even for low-energy impacts, indentation losses must be taken into account, specifically when dealing with polymeric materials [16]. To model these losses a linear dashpot of loss coefficient, c_i, is used. Otherwise, bending, shear and membrane losses may be neglected depending on the material; when considering, an equivalent lumped parameter, c_{eq}, is frequently used [17]. Fig. 1(left) shows the rheological scheme of the complete non-conservative model.

If m_{eff} is very small, when compared to the mass of the striker, it can be neglected. Also, when the plate is relatively thin (the thickness/width ratio is smaller than 0.2), the thin plate theory can be applied and the contribution of shear deformation can be neglected, so $k_b \approx k_{bs}$, which account for bending deformations only. When the deflection of the plate is relatively small (the deflection/thickness ratio is smaller than 0.2), the small deflection theory can be applied and the influence of membrane stretching can be neglected, that is to say, $k_{\mathrm{m}} = 0$ [22]. However, the deflection/thickness ratio in this material was higher than 0.2 for the impact height range herein studied, so the membrane effect was considered. The bending, shear and membrane losses were neglected as a first approximation. Fig. 1(right) shows the rheological scheme of the proposed model for the SRPP.

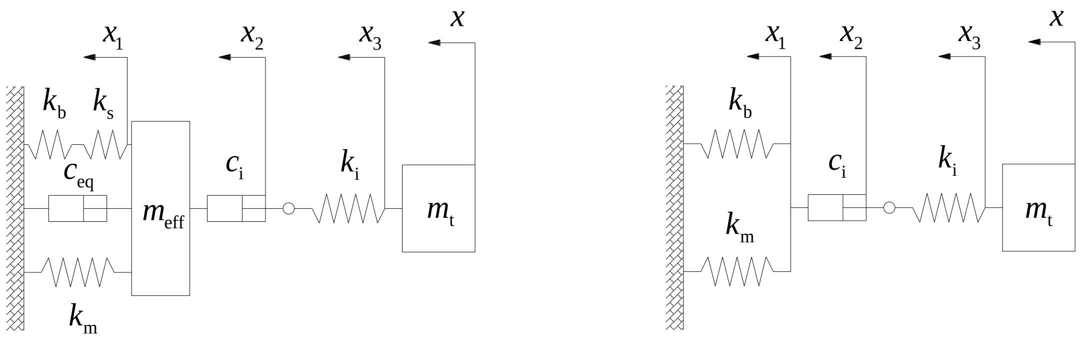

Figure 1. Rheological scheme of (left) the complete non-conservative model and (right) the proposed model.

The proposed model corresponds with a three-degree-of-freedom system whose government equations are given by:

$$m\frac{\mathrm{d}^2 x}{\mathrm{d}t^2} = -k_{\mathrm{i}} x_3^d = -c_{\mathrm{i}}\frac{\mathrm{d}x_2}{\mathrm{d}t} = -\left(k_{\mathrm{b}} x_1 + k_{\mathrm{m}} x_1^3\right) \tag{4}$$

where for a completely clamped isotropic circular plate, the bending and membrane stiffness are respectively given by [22]:

$$k_{\mathrm{b}} = \frac{4\pi E h^3}{3(1-\nu^2)a^2} \tag{5}$$

$$k_{\mathrm{m}} = \frac{(353-191\nu)\pi E h}{648(1-\nu)a^2} \tag{6}$$

where ν is the Poisson ratio, E is the in-plane modulus, h is the plate thickness and a is the radius of the plate. Taking into account the following expression, obtained from the model:

$$x = x_1 + x_2 + x_3 \tag{7}$$

and eliminating x_3, Eq. (3) may be written as:

$$m\ddot{x} = -k_{\mathrm{i}}\left(x - x_1 - x_2\right)^d = -c_{\mathrm{i}}\dot{x}_2 = -\left(k_b x_1 + k_{\mathrm{m}} x_1^3\right) \tag{8}$$

where the operators $(\dot{\bullet})$ and $(\ddot{\bullet})$ denote first and second derivatives with respect to time, respectively. This non-linear differential equation can be solved, for example, by means of Runge-Kutta family algorithms.

When dealing with a material presenting a non-linear elastic phase, in Eq. (5) and Eq. (6) an expression of the modulus depending on the strain must be used. The strain is defined by the deflection of the plate. For example, the radial strain, ε_{r}, of a circular thin membrane (no bending stresses) supporting a uniform load is approximately [23]:

$$\varepsilon_{\mathrm{r}} \approx \frac{2}{3}\frac{w_0^2}{a^2} - \frac{2}{5}\frac{w_0^4}{a^4} \tag{9}$$

where w_0 is the central deflection of the plate. Similarly, an expression which defines the strain of a circular plate supporting any load which causes bending stresses could be deduced, although it would be more complex than the previous one since the strain would depend on the radial position and the position throughout the thickness. More complex, if possible, would be the expression for the case where bending and membrane effects were coupled; this is the case of the response of the material herein studied.

3. Material and methodology

3.1. Material

The material used was a SRPP. This composite material consists of a polypropylene fibre 0º/90º woven reinforcement embedded in a polypropylene matrix. It was supplied by Propex™ and it is known by the trade name of Curv®. It initially performs according to a non-linear elastic behaviour until the beginning of irreversible strain mechanisms, where the tangent modulus in one the principal direction is 4.12 GPa (measured by strain gauge). Its Poisson coefficient is 0.3 and its density is 0.92 g/cm^3 [12].

3.2. Methodology

Indentation and transverse impact tests were carried out on SRPP specimens by using a drop-weight machine (Ceast 9350, Instron). It was equipped with a 20 kN load cell attached to a 20 mm diameter hemispherical tup which registered contact force history. First of all, to determine if a noteworthy strain-rate dependence of the impact response existed, transverse impact tests of equal impact energy (1.8 J and 20 J), but different impact velocity-mass configuration, were performed on plates of different thicknesses to compare their respective force-deflection responses. Based on the resulting non-strain-rate dependence, as later be demonstrated, the study was approached as described below.

Indentation impact tests were performed from heights of 31 mm, 62 mm and 93 mm with a 2.045 kg tup on six 2.7 mm thick stacked plates. This configuration avoided a possible influence caused by the holder’s stiffness. The indentation subsystem, corresponding to the first three equalities of Eq. (4), was solved independently of the global system. k_{i}, c_{i} and d were calculated by numerical curve fitting by least squares to the experimental data of the highest impact height test, i.e. that of 93 mm one. Then, the numerical responses for the rest of the cases were compared with the respective experimental data to validate the parameters of the model of the indentation subsystem. Then, $E_{\mathrm{t}2}$ was deduced from k_{i} by using Eq. (3).

After that, k_{b} and k_{m} were formulated based on Eq. (5) and Eq. (6), respectively. Since these expressions are defined for isotropic or transversely isotropic materials, an equivalent transversely isotropic modulus of the SRPP, which is strain-dependent, was used. Because of the non-linear character of the elastic phase of the material, for a specific plate radius, a polynomial expression of the equivalent strain dependent elastic modulus, based on the deflection, was proposed:

$$E(\varepsilon) = E(\varepsilon(w_0)) = E(w_0) = a_4 w_0^4 + a_3 w_0^3 + a_2 w_0^2 + a_1 w_0 + a_0 \tag{10}$$

where the coefficients were obtained by numerical curve fitting by least squares to the experimental data obtained from one of the transverse impact tests and a_0 corresponded specifically with the equivalent modulus for a null strain, i.e. it coincided with the equivalent tangent modulus.

Finally, bending impact tests were performed from heights of 31 mm, 62 mm and 93 mm with a 2.045 kg tup on plates of 1 mm, 1.34 mm and 1.68 mm thick which were clamped by a 40 mm diameter annular grip. The numerical model, already completely defined, was performed for the different combinations of height and thickness to compare the predicted responses with the experimental data.

4. Results and discussion

First of all, it was analysed if a noteworthy strain-rate dependence of the impact response existed. Fig. 2 shows the force history registered for transverse impact tests of equal impact energy, but obtained from different impact height-mass configurations. The peak forces of the tests of each pair of tests coincided. As it can be seen, both the loads and unloads also coincided, what implied that the expression of the stiffness would remain constant in such impact velocity range, i.e. it was non-strain-rate dependent.

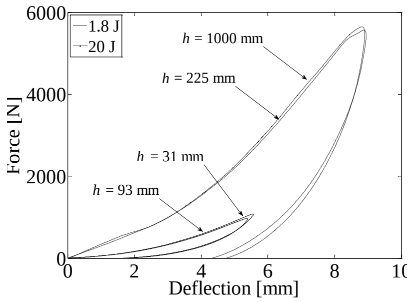

Figure 2. Force history and force-deflection curve for the curves of equal impact energy, but different impact height-mass configurations.

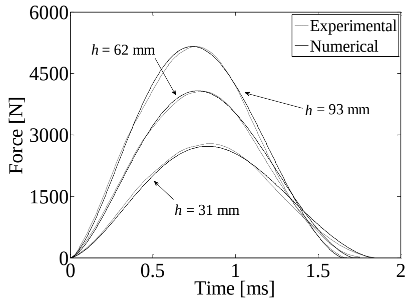

Figure 3. Numerical-experimental correlation of the indentation-impact tests for the different impact heights.

At this point, the indentation model was determined by curve fitting to the experimental data corresponding to the 93 mm impact height test. The mean square error was 1.03% and the resulting parameters were $d = 1.51$, $k_\mathrm{i} = 360 \cdot 10^6$ Nm$^{-1.51}$ and $c_\mathrm{i} = 17 \cdot 10^3$ Nsm^{-1}. The value of the non-linearity coefficient, *d*, resulted in accordance with the Hertz law, which proposes a coefficient of 1.5. According to Eq. (3), $E_{\mathrm{t}2}$ was 1.92 GPa. Fig. 3 shows the numerical-experimental correlation of the indentation-impact tests for the different impact heights.

Once defined the indentation subsystem, to determine the complete model, the force history of a transverse impact curve were fitted based on the parameters of the expression of the equivalent elastic modulus to the experimental data; those of 98 mm impact height on plate of 1.68 mm thick. The variation of the modulus based on the deflection resulted:

$$E(w_0) = -1.302 \cdot 10^3 w_0^4 - 1.120 \cdot 10^2 w_0^3 + 11.93 w_0^2 + 0.2959 w_0 + 2828 \qquad (11)$$

where w_0 is expressed in m and $E(w_0)$ in MPa. As can be seen a_0 resulted 2828 MPa.

Fig. 4 shows the numerical-experimental correlation of the transverse impact tests for the different impact height and plate thicknesses.

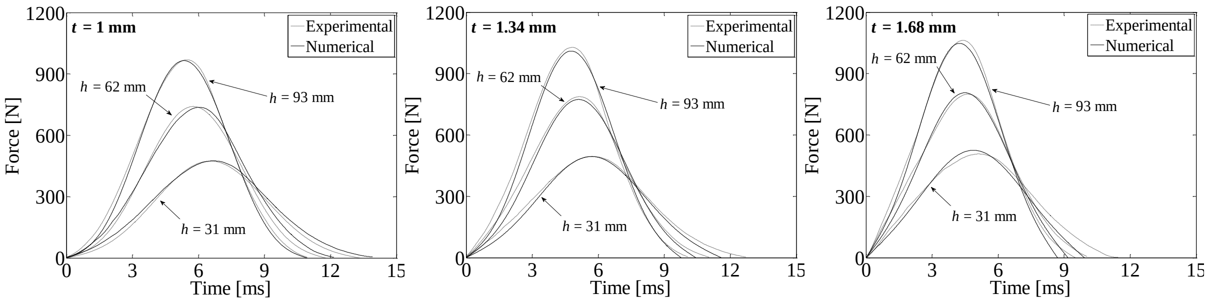

Figure 4. Numerical-experimental correlation of the transverse impact tests for the different impact height and plate thicknesses.

Results show the deduced parameters were valid to predict the indentation impact response in the impact velocity range studied for which the material performed with a E_{t2} of 1.92 GPa. The expression of the equivalent elastic modulus provided an equivalent tangent modulus of 2.82 GPa, coherent with that of the real tangent one of 4.12 GPa corresponding to the orthotropic material.

5. Conclusions

A model to predict the contact force history during low-energy impacts on a self-reinforced polypropylene composite (SRPP) was proposed. The model took into account the local response, i.e. the indentation phenomenon, based on the Hertz theory, and the global response considering bending and membrane effects, based on the plates and shells theory. The SRPP demonstrated negligible strain-rate dependence for the impact velocity range studied and an equivalent elastic modulus formulated as strain dependent, in accordance with the non-linear elastic phase which characterizes the material, was deduced. The results demonstrated that the model was capable of reproducing accurately the low-energy impact response of the material.

References

[1] *European Commission - Official website of the European Commission http://ec.europa.eu/*, 2014.

[2] Directive 2000/53/EC of the European Parliament and of the Council on end-of life vehicles. *Official Journal of the European Communities*, 2000.

[3] A. Kmetty, T. Barany, and J. Karger-Kocsis. Self-reinforced polymeric materials: A review. *Progress in Polymer Science*, 35(10):1288–1310, 2010.

[4] B. Alcock, N.O. Cabrera, N.-M. Barkoula, J. Loos, and T. Peijs. The mechanical properties of unidirectional all-polypropylene composites. *Composites Part A: Applied Science and Manufacturing*, 37(5):716–726, 2006.

[5] B. Alcock, N.O. Cabrera, N.-M. Barkoula, A.B. Spoelstra, J. Loos, and T. Peijs. The mechanical properties of woven tape all-polypropylene composites. *Composites Part A: Applied Science and Manufacturing*, 38(1):147–161, 2007.

[6] J.M. Zhang, C.T. Reynolds, and T. Peijs. All-poly(ethylene terephthalate) composites by film stacking of oriented tapes. *Composites Part A: Applied Science and Manufacturing*, 40(11):1747–1755, 2009.

[7] O.A. Khondker, X. Yang, N. Usui, and H. Hamada. Mechanical properties of textile-inserted pp/pp knitted composites using injection-compression molding. *Composites Part A: Applied Science and Manufacturing*, 37(12):2285–2299, 2006.

[8] Fv. Lacroix, H.-Q. Lu, and K. Schulte. Wet powder impregnation for polyethylene composites: preparation and mechanical properties. *Composites Part A: Applied Science and Manufacturing*, 30(3):369–373, 1999.

[9] Fv. Lacroix, M. Werwer, and K. Schulte. Solution impregnation of polyethylene fibre/polyethylene matrix composites. *Composites Part A: Applied Science and Manufacturing*, 29(4):371–376, 1998.

[10] J. Aurrekoetxea, M. Sarrionandia, M. Mateos, and L. Aretxabaleta. Repeated low energy impact behaviour of self-reinforced polypropylene composites. *Polymer Testing*, 30(2):216–221, 2011.

[11] N.O. Cabrera, C.T. Reynolds, B. Alcock, and T. Peijs. Non-isothermal stamp forming of continuous tape reinforced all-polypropylene composite sheet. *Composites Part A: Applied Science and Manufacturing*, 39(9):1455–1466, 2008.

[12] *Propex Fabrics, Inc. Curv® (self-reinforced Polypropylene, SRPP) http://www.propexbrands.com/*, 2014.

[13] *Lankhorst Pure Composites b.v. PURE® (Self-Reinforced Polypropylene, SRPP) http://www.pure-composites.com/*, 2014.

[14] J.I. Múgica, L. Aretxabaleta, I. Ulacia, and J. Aurrekoetxea. Impact characterization of thermoformable fibre metal laminates of 2024-T3 aluminium and AZ31B-H24 magnesium based on self-reinforced polypropylene. *Composites Part A: Applied Science and Manufacturing*, 61(0):67–75, 2014.

[15] S. Abrate. Modeling of impacts on composite structures. *Composite Structures*, 51(2):129–138, 2001.

[16] O. Jiménez, J.A. Sullcahuaman, M. Sánchez-Soto, and A.B. Martínez. Low energy impact evaluation using non conservative models. *International Journal of Solids and Structures*, 42:5758–5764, 2005.

[17] R.W. Rydin and V.M. Karbhari. Partitioning energy furing low-velocity impact of rtm fiber-reinforced composites. *International Journal of Impact Engineering*, 21(9):773–789, 1998.

[18] L. Rayleigh. XXII. On the production of vibrations by forces of relatively long duration, with application to the theory of collisions. *Philosophical Magazine Series 6*, 11(62):283–291, 1906.

[19] H. Hertz. Über die berührung fester elastischer körper. *Journal für die Reine und Angewandte Mathematik*, 92:156–171, 1881.

[20] L.B. Greszczuk. *Impact Dynamics*, chapter 3, pages 55–95. John Wiley and Sons, Inc., 1982.

[21] J.R. Willis. Hertzian contact of anisotropic bodies. *Journal of the Mechanics and Physics of Solids*, 14(3):163–176, 1966.

[22] S. Timoshenko. *Theory of Plates and Shells*. McGraw-Hill Book Co., 1940.

[23] I.N. Bronštejn, G. Musiol, and H. Mühlig. *Taschenbuch der Mathematik*. Deutsch, 2008.